DESY 00-041
hep-ex/0003018
March 2000

ISSN 0418-9833

Measurement of Inclusive $D_s^{\pm}$ Photoproduction at HERA

ZEUS Collaboration

Abstract

The first measurement of inclusive $D_s^{\pm}$ photoproduction at HERA has been performed with the ZEUS detector for photon-proton centre-of-mass energies $130 < W < 280\,\text{GeV}$. The measured cross section for $3 < p_T^{D_s} < 12\,\text{GeV}$ and $|\eta^{D_s}| < 1.5$ is $\sigma_{ep\to D_s X} = 3.79 \pm 0.59\,(\text{stat.})\,^{+0.26}_{-0.46}\,(\text{syst.}) \pm 0.94\,(\text{br.})\,\text{nb}$, where the last error arises from the uncertainty in the $D_s^{\pm}$ decay branching ratio. The measurements are compared with inclusive $D^{*\pm}$ photoproduction cross sections in the same kinematic region and with QCD calculations. The $D_s^{\pm}$ cross sections lie above a fixed-order next-to-leading order calculation and agree better with a tree-level $O(\alpha\alpha_s^3)$ calculation that was tuned to describe the ZEUS $D^{*\pm}$ cross sections. The ratio of $D_s^{\pm}$ to $D^{*\pm}$ cross sections is $0.41 \pm 0.07\,(\text{stat.})^{+0.03}_{-0.05}\,(\text{syst.}) \pm 0.10\,(\text{br.})$. From this ratio, the strangeness-suppression factor in charm photoproduction, within the LUND string fragmentation model, has been calculated to be $\gamma_s = 0.27 \pm 0.05 \pm 0.07\,(\text{br.})$. The cross-section ratio and γ_s are in good agreement with those obtained in charm production in e^+e^- annihilation.

The ZEUS Collaboration

J. Breitweg, S. Chekanov, M. Derrick, D. Krakauer, S. Magill, B. Musgrave, A. Pellegrino, J. Repond, R. Stanek, R. Yoshida
Argonne National Laboratory, Argonne, IL, USA [p]

M.C.K. Mattingly
Andrews University, Berrien Springs, MI, USA

G. Abbiendi, F. Anselmo, P. Antonioli, G. Bari, M. Basile, L. Bellagamba, D. Boscherini[1], A. Bruni, G. Bruni, G. Cara Romeo, G. Castellini[2], L. Cifarelli[3], F. Cindolo, A. Contin, N. Coppola, M. Corradi, S. De Pasquale, P. Giusti, G. Iacobucci, G. Laurenti, G. Levi, A. Margotti, T. Massam, R. Nania, F. Palmonari, A. Pesci, A. Polini, G. Sartorelli, Y. Zamora Garcia[4], A. Zichichi
University and INFN Bologna, Bologna, Italy [f]

C. Amelung, A. Bornheim, I. Brock, K. Cobö̈ken, J. Crittenden, R. Deffner, H. Hartmann, K. Heinloth, E. Hilger, P. Irrgang, H.-P. Jakob, A. Kappes, U.F. Katz, R. Kerger, E. Paul, H. Schnurbusch, A. Stifutkin, J. Tandler, K.Ch. Voss, A. Weber, H. Wieber
Physikalisches Institut der Universität Bonn, Bonn, Germany [c]

D.S. Bailey, O. Barret, N.H. Brook[5], B. Foster[6], G.P. Heath, H.F. Heath, J.D. McFall, D. Piccioni, E. Rodrigues, J. Scott, R.J. Tapper
H.H. Wills Physics Laboratory, University of Bristol, Bristol, U.K. [o]

M. Capua, A. Mastroberardino, M. Schioppa, G. Susinno
Calabria University, Physics Dept.and INFN, Cosenza, Italy [f]

H.Y. Jeoung, J.Y. Kim, J.H. Lee, I.T. Lim, K.J. Ma, M.Y. Pac[7]
Chonnam National University, Kwangju, Korea [h]

A. Caldwell, W. Liu, X. Liu, B. Mellado, S. Paganis, S. Sampson, W.B. Schmidke, F. Sciulli
Columbia University, Nevis Labs., Irvington on Hudson, N.Y., USA [q]

J. Chwastowski, A. Eskreys, J. Figiel, K. Klimek, K. Olkiewicz, K. Piotrzkowski[8], M.B. Przybycień, P. Stopa, L. Zawiejski
Inst. of Nuclear Physics, Cracow, Poland [j]

B. Bednarek, K. Jeleń, D. Kisielewska, A.M. Kowal, T. Kowalski, M. Przybycień, E. Rulikowska-Zarębska, L. Suszycki, D. Szuba
Faculty of Physics and Nuclear Techniques, Academy of Mining and Metallurgy, Cracow, Poland [j]

A. Kotański
Jagellonian Univ., Dept. of Physics, Cracow, Poland [k]

L.A.T. Bauerdick, U. Behrens, J.K. Bienlein, C. Burgard[9], D. Dannheim, K. Desler, G. Drews, A. Fox-Murphy, U. Fricke, F. Goebel, P. Göttlicher, R. Graciani, T. Haas, W. Hain, G.F. Hartner, D. Hasell[10], K. Hebbel, K.F. Johnson[11], M. Kasemann[12], W. Koch, U. Kötz, H. Kowalski, L. Lindemann[13], B. Löhr, M. Martínez, M. Milite, T. Monteiro[8], M. Moritz, D. Notz, F. Pelucchi, M.C. Petrucci, M. Rohde, P.R.B. Saull, A.A. Savin, U. Schneekloth, F. Selonke, M. Sievers, S. Stonjek, E. Tassi, G. Wolf, U. Wollmer, C. Youngman, W. Zeuner
Deutsches Elektronen-Synchrotron DESY, Hamburg, Germany

C. Coldewey, A. Lopez-Duran Viani, A. Meyer, S. Schlenstedt, P.B. Straub
DESY Zeuthen, Zeuthen, Germany

G. Barbagli, E. Gallo, P. Pelfer
University and INFN, Florence, Italy [f]

G. Maccarrone, L. Votano
INFN, Laboratori Nazionali di Frascati, Frascati, Italy [f]

A. Bamberger, A. Benen, S. Eisenhardt[14], P. Markun, H. Raach, S. Wölfle
Fakultät für Physik der Universität Freiburg i.Br., Freiburg i.Br., Germany [c]

P.J. Bussey, A.T. Doyle, S.W. Lee, N. Macdonald, G.J. McCance, D.H. Saxon, L.E. Sinclair, I.O. Skillicorn, R. Waugh
Dept. of Physics and Astronomy, University of Glasgow, Glasgow, U.K. [o]

I. Bohnet, N. Gendner, U. Holm, A. Meyer-Larsen, H. Salehi, K. Wick
Hamburg University, I. Institute of Exp. Physics, Hamburg, Germany [c]

A. Garfagnini, I. Gialas[15], L.K. Gladilin[16], D. Kçira[17], R. Klanner, E. Lohrmann, G. Poelz, F. Zetsche
Hamburg University, II. Institute of Exp. Physics, Hamburg, Germany [c]

R. Goncalo, K.R. Long, D.B. Miller, A.D. Tapper, R. Walker
Imperial College London, High Energy Nuclear Physics Group, London, U.K. [o]

U. Mallik
University of Iowa, Physics and Astronomy Dept., Iowa City, USA [p]

P. Cloth, D. Filges
Forschungszentrum Jülich, Institut für Kernphysik, Jülich, Germany

T. Ishii, M. Kuze, K. Nagano, K. Tokushuku[18], S. Yamada, Y. Yamazaki
Institute of Particle and Nuclear Studies, KEK, Tsukuba, Japan [g]

S.H. Ahn, S.B. Lee, S.K. Park
Korea University, Seoul, Korea [h]

H. Lim, I.H. Park, D. Son
Kyungpook National University, Taegu, Korea [h]

F. Barreiro, G. García, C. Glasman[19], O. Gonzalez, L. Labarga, J. del Peso, I. Redondo[20], J. Terrón
Univer. Autónoma Madrid, Depto de Física Teórica, Madrid, Spain [n]

M. Barbi, F. Corriveau, D.S. Hanna, A. Ochs, S. Padhi, M. Riveline, D.G. Stairs, M. Wing
McGill University, Dept. of Physics, Montréal, Québec, Canada [a], [b]

T. Tsurugai
Meiji Gakuin University, Faculty of General Education, Yokohama, Japan

V. Bashkirov[21], B.A. Dolgoshein
Moscow Engineering Physics Institute, Moscow, Russia [l]

R.K. Dementiev, P.F. Ermolov, Yu.A. Golubkov, I.I. Katkov, L.A. Khein, N.A. Korotkova, I.A. Korzhavina, V.A. Kuzmin, O.Yu. Lukina, A.S. Proskuryakov, L.M. Shcheglova, A.N. Solomin, N.N. Vlasov, S.A. Zotkin
Moscow State University, Institute of Nuclear Physics, Moscow, Russia [m]

C. Bokel, M. Botje, N. Brümmer, J. Engelen, S. Grijpink, E. Koffeman, P. Kooijman, S. Schagen, A. van Sighem, H. Tiecke, N. Tuning, J.J. Velthuis, J. Vossebeld, L. Wiggers, E. de Wolf
NIKHEF and University of Amsterdam, Amsterdam, Netherlands [i]

D. Acosta[22], B. Bylsma, L.S. Durkin, J. Gilmore, C.M. Ginsburg, C.L. Kim, T.Y. Ling
Ohio State University, Physics Department, Columbus, Ohio, USA [p]

S. Boogert, A.M. Cooper-Sarkar, R.C.E. Devenish, J. Große-Knetter[23], T. Matsushita, O. Ruske, M.R. Sutton, R. Walczak
Department of Physics, University of Oxford, Oxford U.K. [o]

A. Bertolin, R. Brugnera, R. Carlin, F. Dal Corso, U. Dosselli, S. Dusini, S. Limentani, M. Morandin, M. Posocco, L. Stanco, R. Stroili, C. Voci
Dipartimento di Fisica dell' Università and INFN, Padova, Italy [f]

L. Adamczyk[24], L. Iannotti[24], B.Y. Oh, J.R. Okrasiński, W.S. Toothacker, J.J. Whitmore
Pennsylvania State University, Dept. of Physics, University Park, PA, USA [q]

Y. Iga
Polytechnic University, Sagamihara, Japan [g]

G. D'Agostini, G. Marini, A. Nigro
Dipartimento di Fisica, Univ. 'La Sapienza' and INFN, Rome, Italy [f]

C. Cormack, J.C. Hart, N.A. McCubbin, T.P. Shah
Rutherford Appleton Laboratory, Chilton, Didcot, Oxon, U.K. [o]

D. Epperson, C. Heusch, H.F.-W. Sadrozinski, A. Seiden, R. Wichmann, D.C. Williams
University of California, Santa Cruz, CA, USA [p]

N. Pavel
Fachbereich Physik der Universität-Gesamthochschule Siegen, Germany [c]

H. Abramowicz[25], S. Dagan[26], S. Kananov[26], A. Kreisel, A. Levy[26]
Raymond and Beverly Sackler Faculty of Exact Sciences, School of Physics, Tel-Aviv University, Tel-Aviv, Israel [e]

T. Abe, T. Fusayasu, K. Umemori, T. Yamashita
Department of Physics, University of Tokyo, Tokyo, Japan [g]

R. Hamatsu, T. Hirose, M. Inuzuka, S. Kitamura[27], T. Nishimura
Tokyo Metropolitan University, Dept. of Physics, Tokyo, Japan [g]

M. Arneodo[28], N. Cartiglia, R. Cirio, M. Costa, M.I. Ferrero, S. Maselli, V. Monaco, C. Peroni, M. Ruspa, R. Sacchi, A. Solano, A. Staiano
Università di Torino, Dipartimento di Fisica Sperimentale and INFN, Torino, Italy [f]

M. Dardo
II Faculty of Sciences, Torino University and INFN - Alessandria, Italy [f]

D.C. Bailey, C.-P. Fagerstroem, R. Galea, T. Koop, G.M. Levman, J.F. Martin, R.S. Orr, S. Polenz, A. Sabetfakhri, D. Simmons
University of Toronto, Dept. of Physics, Toronto, Ont., Canada [a]

J.M. Butterworth, C.D. Catterall, M.E. Hayes, E.A. Heaphy, T.W. Jones, J.B. Lane, B.J. West
University College London, Physics and Astronomy Dept., London, U.K. [o]

J. Ciborowski, R. Ciesielski, G. Grzelak, R.J. Nowak, J.M. Pawlak, R. Pawlak, B. Smalska, T. Tymieniecka, A.K. Wróblewski, J.A. Zakrzewski, A.F. Żarnecki
Warsaw University, Institute of Experimental Physics, Warsaw, Poland [j]

M. Adamus, T. Gadaj
Institute for Nuclear Studies, Warsaw, Poland [j]

O. Deppe, Y. Eisenberg, D. Hochman, U. Karshon[26]
Weizmann Institute, Department of Particle Physics, Rehovot, Israel [d]

W.F. Badgett, D. Chapin, R. Cross, C. Foudas, S. Mattingly, D.D. Reeder, W.H. Smith, A. Vaiciulis[29], T. Wildschek, M. Wodarczyk
University of Wisconsin, Dept. of Physics, Madison, WI, USA [p]

A. Deshpande, S. Dhawan, V.W. Hughes
Yale University, Department of Physics, New Haven, CT, USA [p]

S. Bhadra, C. Catterall, J.E. Cole, W.R. Frisken, R. Hall-Wilton, M. Khakzad, S. Menary
York University, Dept. of Physics, Toronto, Ont., Canada [a]

[1] now visiting scientist at DESY
[2] also at IROE Florence, Italy
[3] now at Univ. of Salerno and INFN Napoli, Italy
[4] supported by Worldlab, Lausanne, Switzerland
[5] PPARC Advanced fellow
[6] also at University of Hamburg, Alexander von Humboldt Research Award
[7] now at Dongshin University, Naju, Korea
[8] now at CERN
[9] now at Barclays Capital PLC, London
[10] now at Massachusetts Institute of Technology, Cambridge, MA, USA
[11] visitor from Florida State University
[12] now at Fermilab, Batavia, IL, USA
[13] now at SAP A.G., Walldorf, Germany
[14] now at University of Edinburgh, Edinburgh, U.K.
[15] visitor of Univ. of Crete, Greece, partially supported by DAAD, Bonn - Kz. A/98/16764
[16] on leave from MSU, supported by the GIF, contract I-0444-176.07/95
[17] supported by DAAD, Bonn - Kz. A/98/12712
[18] also at University of Tokyo
[19] supported by an EC fellowship number ERBFMBICT 972523
[20] supported by the Comunidad Autonoma de Madrid
[21] now at Loma Linda University, Loma Linda, CA, USA
[22] now at University of Florida, Gainesville, FL, USA
[23] supported by the Feodor Lynen Program of the Alexander von Humboldt foundation
[24] partly supported by Tel Aviv University
[25] an Alexander von Humboldt Fellow at University of Hamburg
[26] supported by a MINERVA Fellowship
[27] present address: Tokyo Metropolitan University of Health Sciences, Tokyo 116-8551, Japan
[28] now also at Università del Piemonte Orientale, I-28100 Novara, Italy
[29] now at University of Rochester, Rochester, NY, USA

[a] supported by the Natural Sciences and Engineering Research Council of Canada (NSERC)
[b] supported by the FCAR of Québec, Canada
[c] supported by the German Federal Ministry for Education and Science, Research and Technology (BMBF), under contract numbers 057BN19P, 057FR19P, 057HH19P, 057HH29P, 057SI75I
[d] supported by the MINERVA Gesellschaft für Forschung GmbH, the German Israeli Foundation, the Israel Science Foundation, the Israel Ministry of Science and the Benozyio Center for High Energy Physics
[e] supported by the German-Israeli Foundation, the Israel Science Foundation, the U.S.-Israel Binational Science Foundation, and by the Israel Ministry of Science
[f] supported by the Italian National Institute for Nuclear Physics (INFN)
[g] supported by the Japanese Ministry of Education, Science and Culture (the Monbusho) and its grants for Scientific Research
[h] supported by the Korean Ministry of Education and Korea Science and Engineering Foundation
[i] supported by the Netherlands Foundation for Research on Matter (FOM)
[j] supported by the Polish State Committee for Scientific Research, grant No. 112/E-356/SPUB/DESY/P03/DZ 3/99, 620/E-77/SPUB/DESY/P-03/ DZ 1/99, 2P03B03216, 2P03B04616, 2P03B03517, and by the German Federal Ministry of Education and Science, Research and Technology (BMBF)
[k] supported by the Polish State Committee for Scientific Research (grant No. 2P03B08614 and 2P03B06116)
[l] partially supported by the German Federal Ministry for Education and Science, Research and Technology (BMBF)
[m] supported by the Fund for Fundamental Research of Russian Ministry for Science and Education and by the German Federal Ministry for Education and Science, Research and Technology (BMBF)
[n] supported by the Spanish Ministry of Education and Science through funds provided by CICYT
[o] supported by the Particle Physics and Astronomy Research Council
[p] supported by the US Department of Energy
[q] supported by the US National Science Foundation

1 Introduction

Inclusive $D_s^\pm$ photoproduction cross sections at HERA are presented for photon-proton centre-of-mass energies in the range $130 < W < 280\,\text{GeV}$. The $D_s^\pm$ mesons were reconstructed through the decay chain $D_s^\pm \to \phi\pi^\pm \to (K^+K^-)\pi^\pm$. This analysis supplements recent measurements of inclusive photoproduction of $D^{*\pm}$ mesons at HERA [1, 2]. The high-statistics measurement by the ZEUS collaboration [1] was performed in the same W range as given above. The measured cross sections were compared to next-to-leading order (NLO) calculations [3, 4, 5] with fragmentation parameters extracted from $D^{*\pm}$ production in e^+e^- annihilation. The experimental results were found generally to lie above the NLO expectations, in particular in the forward (proton) direction.

The study of $D_s^\pm$ photoproduction provides another test of perturbative QCD (pQCD) calculations of charm production [3, 6] which is experimentally independent of the $D^{*\pm}$ measurement. Furthermore, from a ratio of the $D_s^\pm$ and $D^{*\pm}$ cross sections the strangeness-suppression factor, γ_s, in charm fragmentation can be determined. A comparison of the cross-section ratio and γ_s with those obtained in charm production in e^+e^- annihilation tests the universality of charm fragmentation.

2 Experimental Conditions

The measurements were performed at the HERA ep collider in the ZEUS detector during 1996/1997. In this period HERA collided positrons with energy $E_e = 27.5\,\text{GeV}$ and protons with energy $E_p = 820\,\text{GeV}$. The integrated luminosity used in this analysis is $38\,\text{pb}^{-1}$. A detailed description of the detector can be found elsewhere [7].

Charged particles were measured in the central tracking detector, CTD [8], which is a drift chamber consisting of 72 concentric sense-wire layers covering the polar angle[1] region $15° < \theta < 164°$. The CTD operates in a magnetic field of 1.43 T provided by a thin superconducting solenoid. The transverse momentum resolution for full length tracks is $\sigma_{p_\perp}/p_\perp = 0.0058\,p_\perp \oplus 0.0065 \oplus 0.0014/p_\perp$ ($p_\perp$ in GeV). To estimate the energy loss, dE/dx, of tracks, the truncated mean of the sense-wire pulse-heights was recorded for each track, discarding the 10 % lowest and 30 % highest pulses.

The solenoid is surrounded by the uranium–scintillator sampling calorimeter (CAL) [9], which is almost hermetic and consists of 5918 cells, each read out by two photomultipliers. Under test beam conditions, the CAL has a relative energy resolution of $0.18/\sqrt{E}$ (E in GeV) for electrons and $0.35/\sqrt{E}$ for hadrons.

The luminosity was determined from the rate of the bremsstrahlung process $e^+p \to e^+\gamma p$, where the photon was measured by a lead–scintillator calorimeter [10] located at $Z = -107\,\text{m}$.

[1] The ZEUS coordinate system is right-handed and has the nominal interaction point at $X = Y = Z = 0$, with the Z-axis pointing in the proton beam direction and the X-axis horizontal, pointing towards the center of HERA.

3 Event Selection and $D_s^{\pm}$ Reconstruction

The ZEUS detector uses a three-level trigger system [7]. At the first level (FLT), the calorimeter cells were combined to define regional and global sums that were required to exceed various CAL energy thresholds. At the second level (SLT), beam-gas events were rejected by cutting on the quantity $\Sigma_i(E - p_Z)_i > 8\,\text{GeV}$, where the sum runs over all calorimeter cells and p_Z is the Z component of the momentum vector assigned to each cell of energy E. At the third level (TLT), at least one combination of CTD tracks was required to be within wide mass windows around the nominal ϕ and D_s meson[2] mass values, assuming π and K masses as appropriate. The D_s transverse momentum, $p_\perp^{D_s}$, was required to be greater than 2.8 GeV.

Photoproduction events were selected by requiring that no scattered positron was identified in the CAL [11]. The Jacquet–Blondel [12] estimator of W, $W_{\text{JB}} = \sqrt{2E_p\Sigma_i(E - p_Z)_i}$, was required to be between 115 and 250 GeV. The lower limit was due to the SLT requirement, while the upper one suppressed remaining DIS events with an unidentified scattered positron in the CAL [11]. After correcting for detector effects, the most important of which were energy losses in inactive material in front of the CAL and particle losses in the beam pipe [11, 13], this W_{JB} range corresponds to an interval of true W of $130 < W < 280\,\text{GeV}$. Under these conditions, the photon virtuality, Q^2, is limited to values less than $1\,\text{GeV}^2$. The corresponding median Q^2 was estimated from a Monte Carlo (MC) simulation to be about $3 \times 10^{-4}\,\text{GeV}^2$.

The MC sample used for this analysis was prepared with the PYTHIA 6.1 [14] generator. The proportions of direct- and resolved-photon events [15] corresponded to the PYTHIA cross sections ($\approx 50\%$ each), where charm excitation processes were included in the resolved component [1]. The MRSG [16] and GRV-G HO [17] parametrisations were used for the proton and photon structure functions, respectively. The MC events were processed through the standard ZEUS detector- and trigger-simulation programs and through the event reconstruction package used for offline data processing. The data and MC distributions were found to be in good agreement.

The D_s mesons were reconstructed through the decay mode $D_s^{\pm} \to \phi\pi^{\pm}$, which has a branching ratio $B_{D_s\to\phi\pi} = 0.036 \pm 0.009$ [18]. The ϕ was identified via its decay mode $\phi \to K^+K^-$, with $B_{\phi\to K^+K^-} = 0.491 \pm 0.008$ [18]. The analysis was restricted to the pseudorapidity range $-1.5 < \eta^{D_s} < 1.5$, for which the CTD acceptance is high. Here $\eta^{D_s} \equiv -\ln(\tan\frac{\theta}{2})$, where θ is the polar angle with respect to the proton beam direction. The kinematic region in $p_\perp^{D_s}$ was limited to $3 < p_\perp^{D_s} < 12\,\text{GeV}$. The lower cut was required to comply with the $p_\perp^{D_s}$ cut applied at the TLT. The upper cut was due to the limited statistics.

The three D_s decay tracks were required to originate from the event vertex, which was measured with a resolution of 0.4 cm in the Z direction and 0.1 cm in the XY plane. Only tracks with polar angles $20^\circ < \theta < 160^\circ$ and transverse momenta $p_\perp > 0.75$ GeV were considered in the analysis.

The decay of the pseudoscalar D_s meson to the ϕ (vector) plus π (pseudoscalar) final

[2]Here D^* and D_s refer to $D^{*\pm}$ and $D_s^{\pm}$, respectively.

state results in an alignment of the spin of the ϕ meson with respect to the direction of motion of the ϕ relative to the D_s. Consequently, the distribution of $\cos\theta_K^*$, where θ_K^* is the angle between one of the kaons and the pion in the ϕ rest frame, followed a $\cos^2\theta_K^*$ shape, implying a flat distribution for $\cos^3\theta_K^*$. In contrast, the $\cos\theta_K^*$ distribution of the combinatorial background was flat and its $\cos^3\theta_K^*$ distribution peaked at zero. A cut of $|\cos^3\theta_K^*| > 0.15$ suppressed the background by a factor of approximately two while reducing the signal by 15%.

The dE/dx information was used to allow partial K and π separation. For each kaon (pion) candidate a likelihood function $\ell_{K(\pi)} \equiv \exp\{-\frac{1}{2}[(dE/dx)_{\rm meas} - (dE/dx)_{K(\pi)}]^2/\sigma^2\}$ was determined, where $(dE/dx)_{K(\pi)}$ is the expected value for a kaon (pion), and σ is the dE/dx resolution, which is inversely proportional to $\sqrt{n}$, where n is the number of hits entering the truncated mean. The parametrisation for the dE/dx expectation was obtained [19] from a fit to an independent inclusive track sample (Fig. 1a). A normalised likelihood function $L_i \equiv \ell_i/\sum_j \ell_j$ was defined, where the sum extends over the considered particle hypotheses π, K and p. Provided that the number of hits was sufficiently high ($n > 7$), low-likelihood hypotheses were rejected if $\ell_i < 0.05$, unless $L_i > 0.12$. The dE/dx cuts reduced the combinatorial background by approximately 20%. The signal loss was determined by means of a Monte Carlo simulation, using dE/dx parameters obtained from the data. The overall loss was 2.1%.

For the D_s candidates, $p_\perp^{D_s}/E_\perp^{\theta>10^\circ} > 0.18$ was required, where $E_\perp^{\theta>10^\circ}$ is the transverse energy outside a cone of $\theta = 10^\circ$ defined with respect to the proton direction. This cut removed more than 20% of the background while preserving about 95% of the D_s signal, as verified by MC studies.

The $K^+K^-\pi^\pm$ mass distribution with the above cuts is shown in Fig. 1b for events in the ϕ mass range, $1.0115 < M(K^+K^-) < 1.0275\,\text{GeV}$. The fraction of events with more than one entry in the D_s mass region was less than 1%. The mass distribution was fitted to a sum of a Gaussian with the D_s mass and width as free parameters, and an exponential function describing the non-resonant background. In order to avoid a possible contribution from $D^\pm \to \phi\pi^\pm$, the fit was not extended below 1.895 GeV. The fit yielded 339 ± 48 D_s mesons. The mass value obtained was $M_{D_s} = 1967 \pm 2\,\text{MeV}$, in agreement with the PDG value [18]. The width of the signal was $\sigma_{D_s} = 12.5 \pm 1.9\,\text{MeV}$, in agreement with the MC estimation.

A clear ϕ signal is seen in the $M(K^+K^-)$ distribution (Fig. 1c) for the D_s region, $1.94 < M(K^+K^-\pi^\pm) < 2.00\,\text{GeV}$. The fit function for the ϕ was a relativistic P-wave Breit-Wigner with variable mass and a fixed full-width of 4.43 MeV [18], convoluted with a Gaussian function whose width, σ_ϕ, was a free parameter of the fit. The background was parametrised with the functional form $a[M(K^+K^-) - 2m_K]^b$, where m_K is the $K^\pm$ mass. The fit yielded $M(\phi) = 1019.5 \pm 0.3\,\text{MeV}$, in agreement with the PDG value [18], and $\sigma_\phi = 1.7 \pm 0.4\,\text{MeV}$, in agreement with MC estimation. The number of ϕ mesons originating from D_s decays was estimated by a side-band subtraction, and was found to be in good agreement with the number of D_s obtained from the above $M(K^+K^-\pi^\pm)$ fit.

Table 1: The differential cross sections $d\sigma/dp_\perp^{D_s}$ for $|\eta^{D_s}| < 1.5$ and $d\sigma/d\eta^{D_s}$ for $3 < p_\perp^{D_s} < 12\,\text{GeV}$ for the photoproduction reaction $ep \to D_s X$ in various $p_\perp^{D_s}$ and η^{D_s} bins for $Q^2 < 1\ \text{GeV}^2$ and $130 < W < 280\,\text{GeV}$. The $p_\perp^{D_s}$ points are given at the positions of the average values of an exponential fit to the $p_\perp^{D_s}$ distribution in each bin. Statistical and systematic uncertainties are quoted separately; the third error corresponds to the uncertainty in the $D_s \to \phi\pi$ branching ratio.

$p_\perp^{D_s}$ range [GeV]	$\langle p_\perp^{D_s} \rangle_{\text{fit}}$ [GeV]	$d\sigma/dp_\perp^{D_s} \pm \text{stat.} \pm \text{syst.} \pm \text{br.}$ [nb/GeV]
3 – 4	3.46	$2.49 \pm 0.56\ ^{+0.32}_{-0.40}$
4 – 6	4.86	$0.523 \pm 0.127\ ^{+0.058}_{-0.052}$
6 – 12	8.09	$0.079 \pm 0.021\ ^{+0.017}_{-0.020}$
		$\pm 25\%$
η^{D_s} range		$d\sigma/d\eta^{D_s} \pm \text{stat.} \pm \text{syst.} \pm \text{br.}$ [nb]
-1.5 – -0.5		$1.03 \pm 0.38\ ^{+0.09}_{-0.26}$
-0.5 – 0.5		$1.90 \pm 0.35\ ^{+0.20}_{-0.19}$
0.5 – 1.5		$0.92 \pm 0.29\ ^{+0.16}_{-0.17}$
		$\pm 25\%$

4 Measurement of Inclusive D_s Cross Sections

The inclusive D_s cross section is given by:

$$\sigma_{ep\to D_s X} = \frac{N_{D_s}}{A \cdot \mathcal{L} \cdot B_{D_s\to(\phi\to K^+K^-)\pi}} ,$$

where N_{D_s} is the fitted number of D_s mesons, $\mathcal{L}$ is the integrated luminosity, $B_{D_s\to(\phi\to K^+K^-)\pi} = 0.0177 \pm 0.0044$ is the combined $D_s \to (\phi\to K^+K^-)\,\pi$ decay branching ratio and A is the acceptance calculated with the MC sample (Section 3). The MC sample contains all events with the $D_s \to (\phi\to K^+K^-)\pi$ decay channel as well as small admixtures from other D_s decay modes and from other charm particle decays. Thus these contributions were taken into account in the acceptance correction procedure.

The total D_s cross section in the kinematic region $Q^2 < 1\ \text{GeV}^2$, $130 < W < 280\,\text{GeV}$, $3 < p_\perp^{D_s} < 12\,\text{GeV}$ and $-1.5 < \eta^{D_s} < 1.5$ was measured to be $\sigma_{ep\to D_s X} = 3.79 \pm 0.59\,(\text{stat.})\,^{+0.26}_{-0.46}\,(\text{syst.}) \pm 0.94\,(\text{br.})\,\text{nb}$, where the last error is due to the 25% uncertainty in the branching ratio $B_{D_s\to\phi\pi}$. The differential cross sections $d\sigma/dp_\perp^{D_s}$ and $d\sigma/d\eta^{D_s}$ are given in Table 1. In Fig. 2 they are compared with the distributions for the D^* in the same kinematic region. The overall normalisation uncertainty due to the luminosity measurement (1.7%) is not included in the cross section errors.

4.1 Systematic Uncertainties

A detailed study of possible sources of systematic uncertainties was carried out for all measured cross sections by shifting the nominal analysis parameters as described below, taking into account resolution effects. For each variation, except for the first one, which

is due to the fit systematics, the D_s mass and width were fixed to the values found for the nominal cut values. The following sources of systematic errors were considered:

- the uncertainties in the determination of the number of D_s mesons were estimated by using a quadratic polynomial function for the background parametrisation instead of an exponential one and by varying the range of the $K^+K^-\pi^\pm$ mass distribution in the fit procedure;
- to estimate the uncertainties in the tracking procedure, the track selection cuts, including $M(K^+K^-)$ and $\cos\theta^*_K$, were shifted by at least the expected resolutions from the nominal values (Section 3);
- the cut on $p_\perp^{D_s}/E_\perp^{\theta>10^\circ}$ was changed by $\pm 10\%$;
- the MC simulation was found to reproduce the absolute energy scale of the CAL to within $\pm 3\%$ [20]. The corresponding uncertainty in the cross section was calculated, including a shift of 3% in the FLT CAL energy thresholds (Section 3);
- the fraction of resolved photon processes in the PYTHIA MC sample was varied between 40% and 60%;
- the dE/dx likelihood cuts were changed in the range $0.02 < l_i < 0.10$ and $0.08 < L_i < 0.15$;
- the uncertainty associated with the correction to the true W range was determined by moving the $W_{\rm JB}$ boundary values by the estimated resolution of $\pm 7\%$.

None of the above was dominant in the total systematic uncertainty to the inclusive D_s cross section. All systematic errors were added in quadrature, yielding a total uncertainty of $^{+7}_{-12}\%$, compared to a statistical error of 16%.

5 Comparison with QCD Calculations

The D_s cross sections were compared to two types of pQCD calculations [3, 6]. The fractions of c quarks hadronising as D^* and D_s mesons were used as input to each calculation. The values $f(c \to D^{*+}) = 0.235 \pm 0.007\,(\pm 0.007)$ and $f(c \to D_s^+) = 0.101 \pm 0.009\,(\pm 0.025)$ were extracted [21] by a least-squares procedure from all relevant existing e^+e^- experimental data [22]. The errors in brackets are due to uncertainties in the charm hadron decay branching ratios. They affect experimental and theoretical cross-section calculations in the same way and can be ignored in the comparison.

The NLO calculation of charm photoproduction in the fixed-order approach of Frixione et al. [3] assumes that gluons and light quarks (u, d, s) are the only active partons in the structure functions of the proton and the photon. In this approach there is no explicit charm excitation component, which can be important in charm photoproduction at HERA [1], and charm is only produced dynamically in hard pQCD processes. This

calculation is expected to be valid when the c-quark transverse momentum, $p_\perp$, is not much larger than the c-quark mass, m_c.

The structure function parametrisations used in the NLO calculation were MRSG [16] for the proton and GRV-G HO [17] for the photon. The renormalisation scale used was $\mu_R = m_\perp \equiv \sqrt{m_c^2 + p_\perp^2}$, and the factorisation scales of the photon and proton structure functions were set to $\mu_F = 2m_\perp$. The pole mass definition is used in this calculation for the c-quark mass with a nominal value $m_c = 1.5\,\text{GeV}$. The Peterson fragmentation function [23] was used for charm fragmentation in this calculation. The Peterson parameter $\epsilon = 0.035$ was obtained for D^* in a NLO fit [24] to ARGUS data [22]. A recent NLO fit [25] to ARGUS data yields an $\epsilon(D_s)$ value equal to $\epsilon(D^*)$ within the fit uncertainties. Using the same value for both channels leads to the same predictions, except for the difference in $f(c \to D^{*+})$ and $f(c \to D_s^+)$, which enter the calculation as scale factors. The NLO prediction for the total inclusive D_s cross section of 2.18 nb is smaller by ≈ 2 standard deviations compared to the measured cross section. Scaling the Peterson parameter ϵ with the squared ratio of the constituent quark masses [23], $m_s = 0.5\,\text{GeV}$ and $m_{u,d} = 0.32\,\text{GeV}$ [26], leads to $\epsilon(D_s) = 0.085$, which yields a NLO prediction 22% lower than that with $\epsilon(D_s) = 0.035$.

In Fig. 2, the NLO calculations are compared to the differential cross sections. The thick curves correspond to the nominal values of μ_R and m_c, as defined above. For the thin curves, a rather extreme value for the c-quark mass, $m_c = 1.2\,\text{GeV}$, and a μ_R value of $0.5m_\perp$ have been used. The D_s cross section decreases steeply with rising $p_\perp$, as in the D^* case. The NLO calculation reproduces within errors the shape of the $p_\perp^{D_s}$ distribution but underestimates the data for the nominal parameter set. For the η^{D_s} distribution the NLO predictions are below the data in the central and forward regions. A similar effect was observed when $d\sigma/d\eta^{D^*}$ distributions were compared with various NLO predictions over a wide range of W values and photon virtualities [1, 27, 28].

Recently Berezhnoy, Kiselev and Likhoded (BKL) have suggested another model [6] which does not employ any specific fragmentation function. In this tree-level pQCD $O(\alpha\alpha_s^3)$ calculation, the $(c, \bar{q})$ state produced in pQCD is hadronised, taking into account both colour-singlet and colour-octet contributions. Using the experimental value for $f(c \to D^{*+})$, a c-quark mass $m_c = 1.5\,\text{GeV}$, a light constituent quark mass $m_q = 0.3\,\text{GeV}$ and the CTEQ4M proton structure function parametrisation [29], the ratio of the colour-octet and colour-singlet components was tuned to describe the ZEUS D^* photoproduction cross sections [1].[3] This ratio and the experimental value for $f(c \to D_s^+)$ were used to obtain predictions for D_s photoproduction. In this case, a strange quark mass, $m_s = 0.5\,\text{GeV}$, was used instead of m_q. The calculated cross sections for D_s and ${D_s}^{*\pm}$ were combined, since the inclusive D_s channel includes fully the prompt ${D_s}^{*\pm}$ meson production.

In Fig. 3, the BKL calculations are compared to the D_s differential cross-section measurements. The agreement with the data is better than that of the NLO calculation with the nominal parameters, but the shape of the η^{D_s} distribution is not matched by the BKL prediction. The total predicted D_s cross section in the kinematic range of the measurement (3.37 nb) is compatible with the measured inclusive cross section.

[3] A comparison of the D^* data with the BKL calculations can be found in the BKL paper [6].

6 D_s to D^* cross-section ratio and γ_s

In the D_s kinematic region, as defined in Section 4, the D^* cross section was measured to be $\sigma_{ep\to D^*X} = 9.17 \pm 0.35\,(\text{stat.})\,^{+0.40}_{-0.39}\,(\text{syst.})$ nb [1]. This yields a ratio $\sigma_{ep\to D_sX}/\sigma_{ep\to D^*X} = 0.41 \pm 0.07\,(\text{stat.})^{+0.03}_{-0.05}\,(\text{syst.}) \pm 0.10\,(\text{br.})$, where common systematic errors (W_{JB} and CAL energy scale) have been removed and the last error is the uncertainty in $B_{D_s\to\phi\pi}$. This ratio is in good agreement with the ratio $f(c \to D_s^+)/f(c \to D^{*+}) = 0.43 \pm 0.04 \pm 0.11\,(\text{br.})$ obtained from results of e^+e^- experiments (see Section 5). The last error originates from the uncertainty in $B_{D_s\to\phi\pi}$ and can be ignored in the comparison.

The strangeness-suppression factor, γ_s, is the ratio of probabilities to create s and u, d quarks during the fragmentation process. In simulation programs based on the Lund string fragmentation scheme [26], γ_s is a free parameter with a default value of 0.3. By varying the value of γ_s in the PYTHIA simulation [14], a direct relation can be obtained between γ_s and the D_s to D^* cross-section ratio. Fixing the value of $f(c \to D^{*+})$ in PYTHIA to 0.235 [21] yields

$$\gamma_s = 0.27 \pm 0.04\,(\text{stat.})\,^{+0.02}_{-0.03}\,(\text{syst.}) \pm 0.01\,(\text{frac.}) \pm 0.07\,(\text{br.})\ .$$

The third error is due to the uncertainty in $f(c \to D^{*+})$, while the forth one results from the uncertainty in $B_{D_s\to\phi\pi}$. Adding all errors in quadrature, except the last one, gives $\gamma_s = 0.27 \pm 0.05 \pm 0.07\,(\text{br.})$.

Previously, γ_s was measured mainly from the ratio of K to π production and from the momentum spectrum of K mesons in hadron-hadron [30, 31] and e^+e^- [32, 33, 34] collisions, as well as in deep inelastic scattering (DIS) experiments [35, 36, 37]. The most accurate measurement, obtained in $p\bar{p}$ collisions [31], is $\gamma_s = 0.29 \pm 0.02\,(\text{stat.}) \pm 0.01\,(\text{syst.})$. The DIS results require a lower value, $\gamma_s \approx 0.2$. Recent results from e^+e^- collisions are in some disagreement with each other. The SLD preliminary result [33] is $\gamma_s = 0.26 \pm 0.06$, while OPAL finds [34] $\gamma_s = 0.422 \pm 0.049 \pm 0.059$. Previous γ_s measurements are therefore in good agreement with that of this analysis, except the latest OPAL value, which is about 2 standard deviations higher.

Existing γ_s values obtained from heavy-meson production (charm and beauty) in e^+e^- collisions [32] are centred around 0.3. For charm production, the ratio $2f(c \to D_s^+)/[f(c \to D^+) + f(c \to D^0)]$ was used as a measure of γ_s. Using for the above fractions the more recent values quoted in [21] leads to $\gamma_s = 0.26 \pm 0.03 \pm 0.07\,(\text{br.})$, where the latter uncertainty originates from $B_{D_s\to\phi\pi}$ and can be ignored in the comparison with the ZEUS result.

The results presented here on the D_s to D^* cross-section ratio and on γ_s, taken together with charm production data in e^+e^- annihilation, tend to support the universality of charm fragmentation.

7 Summary and Conclusions

The first measurement at HERA of inclusive ${D_s}^{\pm}$ photoproduction has been performed with the ZEUS detector. The cross section for $Q^2 < 1\,\text{GeV}^2$, $130 < W < 280\,\text{GeV}$,

$3 < p_\perp^{D_s} < 12\,\text{GeV}$ and $-1.5 < \eta^{D_s} < 1.5$ is $\sigma_{ep\to D_s X} = 3.79 \pm 0.59\,(\text{stat.})\,^{+0.26}_{-0.46}\,(\text{syst.}) \pm 0.94\,(\text{br.})\,\text{nb}$. The differential cross sections $d\sigma/dp_\perp^{D_s}$ and $d\sigma/d\eta^{D_s}$ are generally above fixed-order NLO calculations, as was the case with the results previously obtained for D^* photoproduction in the same kinematic region. The BKL calculation, using the octet-to-singlet ratio tuned to fit the ZEUS D^* data, describes the D_s cross sections reasonably well, but the shape of the η^{D_s} distribution is not matched by the BKL prediction. The cross-section ratio, $\sigma_{ep\to D_s X}/\sigma_{ep\to D^* X}$, in the kinematic region as defined above is $0.41 \pm 0.07\,(\text{stat.})^{+0.03}_{-0.05}\,(\text{syst.}) \pm 0.10\,(\text{br.})$, in good agreement with the ratio of c quarks hadronising into D_s and D^* mesons, extracted from e^+e^- experiments. From this ratio, the strangeness-suppression factor in charm photoproduction, within the LUND string fragmentation model, has been calculated to be $\gamma_s = 0.27 \pm 0.04\,(\text{stat.})\,^{+0.02}_{-0.03}\,(\text{syst.}) \pm 0.01\,(\text{frac.}) \pm 0.07\,(\text{br.})$, in good agreement with the γ_s value extracted from charm production in e^+e^- annihilation.

8 Acknowledgements

We would like to thank the DESY Directorate for their strong support and encouragement. The remarkable achievements of the HERA machine group were essential for the successful completion of this work and are greatly appreciated. We would like to thank C. Oleari for discussions and for providing us with his latest results for $\epsilon(D_s)$ and S. Frixione and A. Berezhnoy for providing us with their QCD calculations.

References

[1] ZEUS Collaboration, J. Breitweg et al., Eur. Phys. J. C6 (1999) 67.

[2] H1 Collaboration, C. Adloff et al., Nucl. Phys. B545 (1999) 21.

[3] S. Frixione et al., Nucl. Phys. B454 (1995) 3; Phys. Lett. B348 (1995) 633.

[4] B.A. Kniehl et al., Z. Phys. C76 (1997) 689;
J. Binnewies et al., Z. Phys. C76 (1997) 677; Phys. Rev. D58 (1998) 014014.

[5] M. Cacciari et al., Phys. Rev. D55 (1997) 2736; ibid., D55 (1997) 7314.

[6] A.V. Berezhnoy, V.V. Kiselev, and A.K. Likhoded, hep-ph/9901333, hep-ph/9905555, Yad. Fiz. [Phys. At. Nucl.] in print (2000).

[7] ZEUS Collaboration, M. Derrick et al., Phys. Lett. B293 (1992) 465;
The ZEUS Detector: Status Report 1993, DESY 1993.

[8] N. Harnew et al., Nucl. Inst. Meth. A279 (1989) 290;
B. Foster et al., Nucl. Phys. Proc. Suppl. B32 (1993) 181;
B. Foster et al., Nucl. Inst. Meth. A338 (1994) 254.

[9] M. Derrick et al., Nucl. Inst. Meth. A309 (1991) 77;
A. Andresen et al., ibid., A309 (1991) 101;
A. Caldwell et al., ibid., A321 (1992) 356;
A. Bernstein et al., ibid., A336 (1993) 23.

[10] J. Andruszków et al., DESY 92-066, 1992;
ZEUS Collaboration, M. Derrick et al., Z. Phys. C63 (1994) 391.

[11] ZEUS Collaboration, M. Derrick et al., Phys. Lett. B322 (1994) 287.

[12] F. Jacquet and A. Blondel, Proc. of the Study for an *ep* Facility for Europe, ed. U. Amaldi, DESY 79/48 (1979) 377.

[13] ZEUS Collaboration, M. Derrick et al., Phys. Lett. B349 (1995) 225.

[14] T. Sjöstrand, Comp. Phys. Commun. 82 (1994) 74.

[15] J.F. Owens, Phys. Rev. D21 (1980) 54;
M. Drees and F. Halzen, Phys. Rev. Lett. 61 (1988) 275;
M. Drees and R.M. Godbole, Phys. Rev. D39 (1989) 169.

[16] A.D. Martin, W.J. Stirling and R.G. Roberts, Phys. Lett. B354 (1995) 155.

[17] M. Glück, E. Reya and A. Vogt, Phys. Rev. D46 (1992) 1973.

[18] C. Caso et al., Particle Data Group, Eur. Phys. J. C3 (1998) 1.

[19] O. Deppe, PhD Thesis, Univ. Hamburg 1999, DESY-THESIS-2000-006.
Earlier dE/dx studies were performed by R.J. Teuscher, PhD Thesis, Univ. Toronto 1997, Internal Report DESY F35D-97-01.

[20] ZEUS Collaboration, M. Derrick et al., Z. Phys. C72 (1996) 399.

[21] L. Gladilin, hep-ex/9912064, 1999.

[22] ARGUS Collaboration, H. Albrecht et al. Z. Phys. C52 (1991) 353;
ibid., C54 (1992) 1;
CLEO Collaboration, D. Bortoletto et al., Phys. Rev. D37 (1988) 1719;
OPAL Collaboration, K. Ackerstaff et al., Eur. Phys. J. C1 (1998) 439; G. Alexander et al., Z. Phys. C72 (1996) 1;
ALEPH Collaboration, R. Barate et al., hep-ex/9909032, submitted to Eur. Phys. J. C (1999);
DELPHI Collaboration, P. Abreu et al., CERN-EP/99-67, submitted to Eur. Phys. J. C (1999); D. Bloch et al., DELPHI-98-120, paper 122, ICHEP98 Conference Vancouver, Canada, July 1998.

[23] C. Peterson et al., Phys. Rev. D27 (1983) 105.

[24] P. Nason and C. Oleari, Phys. Lett. B447 (1999) 327 and hep-ph/9903541.

[25] C. Oleari, private communication.

[26] T. Sjöstrand, Comp. Phys. Commun. 39 (1986) 347;
T. Sjöstrand and M. Bengtsson, Comp. Phys. Commun. 43 (1987) 367.

[27] ZEUS Collaboration, Paper 525 submitted to the International Europhysics Conference on High Energy Physics 99, Tampere, Finland, July 1999.

[28] ZEUS Collaboration: J. Breitweg et al., Eur. Phys. J. C12 (2000) 35.

[29] H.L. Lai et al., Phys. Rev. D55 (1997) 1280.

[30] A.K. Wroblewski, Proc. of the 25th International Conference on HEP, Singapore (1990) 125.

[31] UA1 Collaboration, G. Bocquet et al., Phys. Lett. B366 (1996) 447.

[32] For a compilation up to 1995 see I.G. Knowles, T. Sjöstrand (convs.) et al., in *Physics at LEP2,* CERN 96-01, Vol.2, p.112, eds. G. Altarelli, T. Sjöstrand and F. Zwirner.

[33] SLD Collaboration, hep-ex/9908033 preprint, submitted to EPS99, Tampere, Finland and to Lepton Photon 99, Stanford, USA.

[34] OPAL Collaboration, hep-ex/0001054 preprint, submitted to Eur. Phys. J. C (2000).

[35] G.T. Jones et al., Z. Phys. C27 (1985) 43;
V. Ammosov et al., Phys. Lett. B93 (1980) 210;
EMC Collaboration, M. Arneodo et al., Z. Phys. C34 (1987) 283 and Phys. Lett. B145 (1984) 156;
N.J. Barker et al., Phys. Rev. D34 (1986) 1251.

[36] E665 Collaboration, M.R. Adams et al., Z. Phys. C61 (1994) 539.

[37] ZEUS Collaboration, M. Derrick et al., Z. Phys. C68 (1995) 29;
H1 Collaboration, S. Aid et al., Nucl. Phys. B480 (1996) 3.

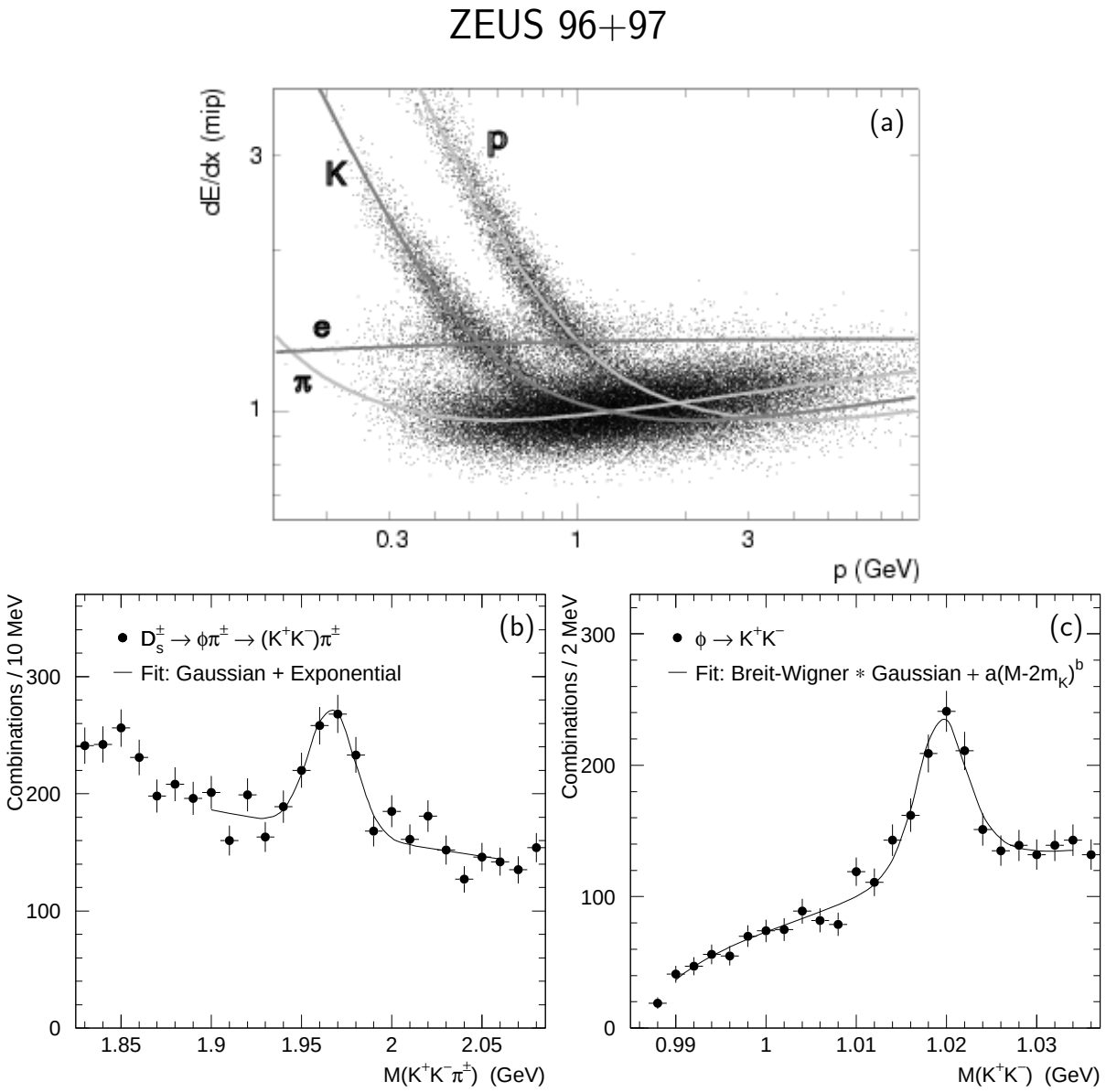

Figure 1: (a) Distribution of the sample used for fitting the dE/dx parametrisation in the $(dE/dx, p)$ plane. Here dE/dx is normalised to a minimum ionizing particle (MIP), defined as the average truncated mean of pion tracks in the momentum range $0.3 < p < 0.4\,\text{GeV}$. The lines indicate the fit result [19]. (b) $M(K^+K^-\pi^{\pm})$ distribution for events inside the ϕ mass range $(1.0115 < M(K^+K^-) < 1.0275\,\text{GeV})$. The solid curve is a fit to a Gaussian (representing the resonance) plus an exponential background. (c) $M(K^+K^-)$ distribution for events inside the D_s mass range $(1.94 < M(K^+K^-\pi^{\pm}) < 2.00\,\text{GeV})$. The solid curve is a fit to a Breit-Wigner convoluted with a Gaussian-shaped resonance and a background parametrisation of the form $a[M(K^+K^-) - 2m_K]^b$.

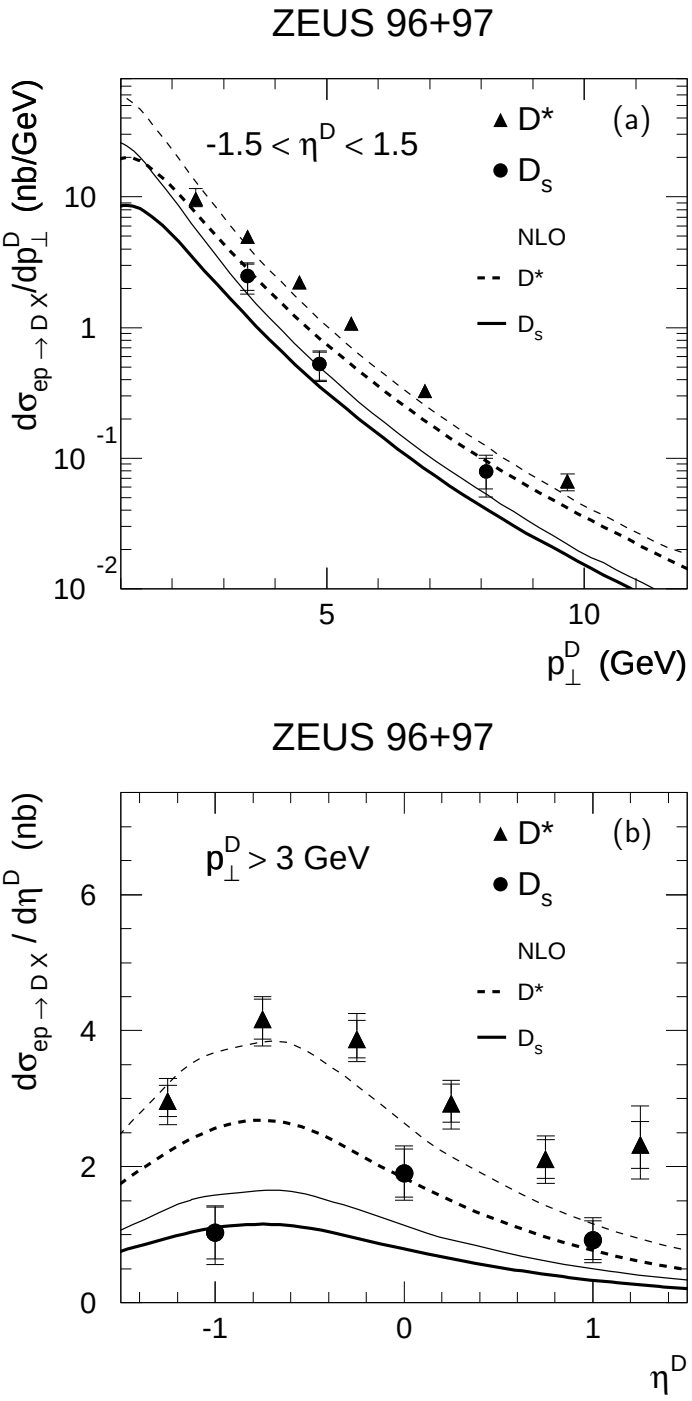

Figure 2: Differential cross sections for the photoproduction reaction $ep \to D\,X$: (a) $d\sigma/dp_\perp^D$ and (b) $d\sigma/d\eta^D$, where D stands for D^* or D_s. The $p_\perp^D$ points are drawn at the position of the average value of an exponential fit in each bin. The η^D points are drawn at the middle of each bin. The inner error bars show the statistical uncertainty, while the outer ones show the statistical and systematic errors added in quadrature. Normalisation uncertainties due to the $D_s \to \phi\pi$ branching ratio are not included in the systematic errors or in the theoretical calculations. The D_s (dots) and D^* (triangles) data are compared with the NLO predictions for D_s (full curves) and D^* (dashed curves) with two parameter settings: $m_c = 1.5\,\mathrm{GeV}$, $\mu_R = m_\perp$ (thick curves) and $m_c = 1.2\,\mathrm{GeV}$, $\mu_R = 0.5 m_\perp$ (thin curves).

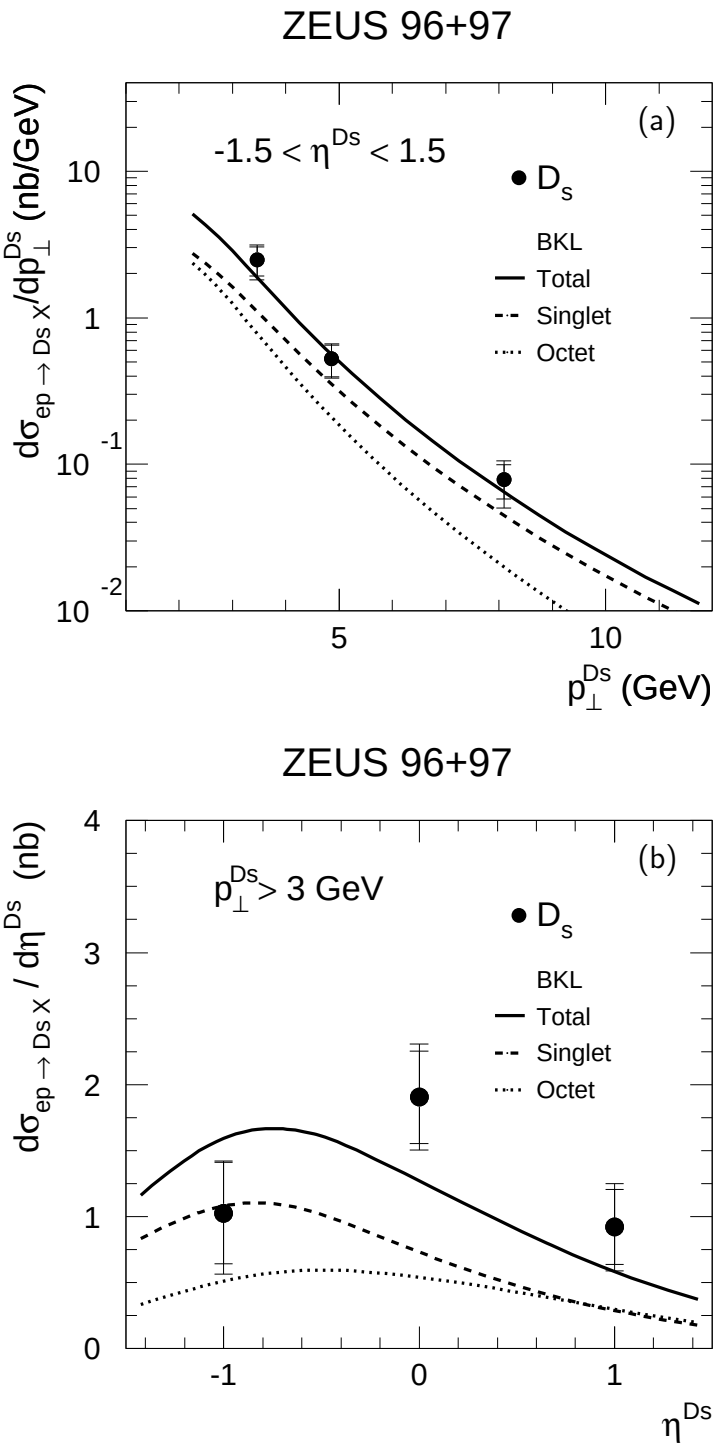

Figure 3: Differential cross sections for the photoproduction reaction $ep \to D_s X$: (a) $d\sigma/dp_\perp^{D_s}$ and (b) $d\sigma/d\eta^{D_s}$ compared to the BKL model [6]. Colour-singlet (dashed curves) and colour-octet (dotted curves) contributions are plotted separately. Their sum is shown as the full curves. The $p_\perp^{D_s}$ points are drawn at the position of the average value of an exponential fit in each bin. The η^{D_s} points are drawn at the middle of each bin. The inner error bars show the statistical uncertainty, while the outer ones show the statistical and systematic errors added in quadrature. Normalisation uncertainties due to the $D_s \to \phi\pi$ branching ratio are not included in the systematic errors or in the theoretical calculations.